On-chip intermediate LED-IF based detection for the control of electromigration in multi-channel networks for isotachophoretic and capillary electrophoretic separations

Daniel Sydes[a], Pablo A. Kler[a,b], Hans Meyer[c], Peter Zipfl[d], Daniel Lutz[e], Carolin Huhn[a]

[a]Institute of Physical and Theoretical Chemistry, Faculty of Science, Eberhard Karls Universität Tübingen, Germany, [b]CIMEC, Centro de Investigación de Métodos Computacionales (UNL-CONICET), Santa Fe, Argentina, [c]J&M Anaytik AG, [d]Optoelectronics and Laser Technology Department, University of Applied Sciences Aalen, Aalen, Germany, [e]CalvaSens GmbH, Aalen, Germany.

Keywords
Glass microchip, On-chip LED-IF detection, Isoelectric focusing, Voltage-switching, Two-dimensional separations

Abstract
Monitoring analytes during the transfer step from the first to the second dimension in multidimensional electrophoretic separations is crucial to determine and control the optimal time point for sample transfer and thus to avoid band broadening or unwanted splitting of the sample band with consequent sample loss. A spatially-resolved intermediate on-chip LED-IF detection system was successfully implemented for a hybrid capillary-chip glass interface. The setup includes a high power 455 nm LED prototype as excitation light source and a linear light fiber array consisting of 23 100 µm light fibers for spatially-resolved fluorescence detection in combination with a push broom imager for hyperspectral detection. Using a basic FITC solution, the linear working range was determined to be 0.125 to 25 µg/ml for a single light guide and the absolute detection limit was 0.04 fmol at a signal to noise ratio of 4. With the setup presented here CIEF-focused labeled ß-lactoglobulin was detectable on-chip with a sufficient intensity to monitor the analyte band transfer in the glass chip interface demonstrating its applicability for full or intermediate on-chip detection.

Introduction

For multidimensional electrophoretic separations with sample heart-cutting, monitoring the analyte during the transfer step from the first to the second separation dimension is crucial to determine the optimal time point for sample band transfer to precisely control the sampling step and thus to avoid band broadening or unwanted splitting of the sample band and sample loss [1]. In general, all non-destructive detection methods normally used in capillary electrophoretic separations are applicable as intermediate detection methods, e.g. absorption or fluorescence detection. Considering the low detection volumes (nl-range) in capillary electrophoresis due to the small capillary inner diameters, laser induced fluorescence (LIF) detection is well suited due to high light intensities and ease of focusing also into small volumes as well as its inherently high sensitivity and selectivity, especially when analytes are derivatized [2]. As excitation light sources Nd:YAG (266/355/532 nm), He-Cd (325/442 nm), argon ion (488/514.5 nm), and He-Ne (543.5 nm) lasers are often used [3-13] reaching detection limits in the range of zeptomoles [14]. Classical fluorescence detection setups (using a laser or LED as excitation source) usually require complex optical instrumentation, as well as labeled analytes, although some target molecules exhibit native fluorescence, e.g. at wavelengths in the UV range [15]. With a special interest in the miniaturization of capillary

electrophoretic assays, the use of laser diodes as well as light emitting diodes (LEDs) [6,9,16] gains popularity due to their small size, long lifetime, low power consumption and low costs, despite some sensitivity impairment because of less efficient light focusing [17-19]. Nowadays, LEDs are covering much of the UV-visible and parts of near-infrared spectral regions (280-1300 nm), giving rise to a wide spectrum of potential applications.
For the collection and guidance of the fluorescence light to the detector, lenses, light guides but also fiber arrays can be used. There are three general geometries for fluorescence detection setups: 1) collinear or confocal-types using microscopy optics, 2) right-angle or orthogonal setups using lenses or optical fibers, and 3) bevel angle arrangements with the excitation light focused at angles of 45° or 30° and fluorescence detection perpendicular to the chip surface [9,12,20,21]. In general, scattered excitation light, reflections and refraction from the cover plate and channel walls, Rayleigh and Raman scattering from the sample and background fluorescence from optical lenses and the chip are responsible for increased background signals and therefore low signal to noise ratios (SNR). Fu et al. [12] demonstrated via simulations and experimental data that for a perpendicular excitation setup best SNR were obtained for collection angles of the fluorescence light of 45° and 135°. Furthermore, the use of filter combinations for excitation and fluorescence light such as bandpass and long pass filters generally increases SNR due to decreased background fluorescence from the lenses and the chip substrate. In general, short channel-to-surface as well as excitation source-to-channel distances are most beneficial for increased detection signals [22]. Photodiodes and photomultipliers are commonly used for detection [6,22,23] or - if wavelength-resolved detection is of interest - charge-coupled device (CCD) cameras and diode array detectors (DAD) [3,24,25]. New developments implement hyperspectral imaging using a push broom imager to simultaneously obtain spectral and spatial information of a certain sample area [26]. The advantage of the spatially-resolved over single-point detection is that the movement of a sample plug through a separation channel segment can be monitored in greater detail, such as successfully applied for whole-column monitoring in capillary isoelectric focusing [27].
We here show LED-induced fluorescence (LED-IF) detection for wavelength and spatially-resolved analyte and channel imaging in electrophoretic separation techniques, where a light fiber array covering a channel length of 1 cm is combined with push broom detection. This setup enables the spatially-resolved continuous monitoring of analytes inside a microfluidic chip used as interface for two-dimensional electrophoretic separations.

Materials and Methods

Chemicals

Carrier ampholyte solution Pharmalyte 3–10 for isoelectric focusing was purchased from GE Healthcare Bio-Sciences AB (0.36 meq/mL pH, Uppsala, Sweden). β-Lactoglobulin (β-Lact, bovine milk > 90%, pI: 4.83–5.4, 18.4 kDa), 3-glycidoxypropyl-trimethoxysilane (GPTMS, 97%) and sodium tetraborate decahydrate ($Na_2B_4O_7$) were purchased from Sigma-Aldrich (Steinheim, Germany) and isopropanol (LC-MS grade) from Fluka (Steinheim, Germany). Acetic acid (glacial, 100 %) and hydroxyethyl cellulose (HEC, for synthesis) were from Merck (Darmstadt, Germany), sodium hydroxide (0.1 mol/l, for analysis) was used from AppliChem (Darmstadt, Germany) and methanol (HPLC gradient Grade) from BDH Prolabo Chemicals VWR (Darmstadt, Germany). Triethylamine (TEA,

99%) was purchased from Alfa Aesar (Karlsruhe, Germany). All solutions were prepared with doubly-deionized water (Milli-Q purification system from Millipore, Bedford, MA).

General instrumentation

All electrophoretic separations and flushing experiments were performed using an Agilent 7100 CE system (Agilent Technologies, Waldbronn, Germany) providing pressure and voltage regimes, injection control, and vial handling. MS detection was achieved using an Agilent 6100 Series Single Quadrupole system (Agilent Technologies, Palo Alto, USA). The CE was coupled to the MS via a coaxial sheath liquid interface from Agilent using an Agilent isocratic pump 1260 (Agilent Technologies, Waldbronn, Germany) for delivering sheath liquid (50:50 (v/v) mixture of water and isopropanol, containing 0.1 % acetic or formic acid (matching the background electrolyte counterion) at a constant volume rate of 4 µl/min. Nebulizer pressure was set to 0.28 bar and the drying gas was delivered at rate of 4 l/min at a temperature of 300 °C. The fragmentor was set to +150 V, the capillary voltage was +4 kV and the nozzle voltage +2 kV. The single quadrupole was used in single ion mode (SIM) and scanning mode (scan). The corresponding modes and related m/z are given in the respective figure legends.

Instrumentation for intermediate on-chip LED-IF detection

The LED prototype as well as its control software were developed and fabricated in cooperation with FutureLED (Berlin, Germany), details are given in Table S1 in the supporting information. For tempering the LED, a Peltier element from head electronic (Prien am Chiemsee, Germany) was used. The fluorescence light was collected via a linear fiber array fabricated at art photonics (Berlin, Germany). The push broom imager used for hyperspectral detection of the fluorescence light and the push broom software for signal data recording (Version 1.0) were from J&M Analytik AG (Essingen, Germany). The respective conditions and parameters for measurements using the push broom imager are listed in the figure legends.
The following optical elements were used and purchased from J&M Analytik AG: (i) collector lens: PCX cylindrical lens, uncoated, focal length 25 mm, 12.5 mm diameter; (ii) slit focusing lens: plano-convex lens focal length 15 mm; (iii) band pass filter for band width reduction of LED emission: band pass filter 452 nm, 51 nm FWHM, OD >6.0 Coating Performance, OD6 blocking, 12.5 mm diameter; (iv) cut off filter for excitation light: long pass filter 500 nm, OD >4, 12.5 mm diameter.
The push broom imager included a QSI 620i 2.0mp cooled CCD camera from Quantum Scientific Imaging (Poplarville, USA). For the spectrograph (J&M Analytik AG, Essingen, Germany) we included a slit for optimal optical filters (filter size 2.0 × 12.5 mm). The technical parameters of the push broom imager are summarized in supplementary material (Table S2). The width of the entrance slit of the spectrograph was 14 mm.

Chip interface

Following previous studies [28,29] a microfluidic borofloat glass chip interface (iX-factory GmbH, Dortmund, Germany) with double T or cross channel layout was used. Channels cross sectional dimensions are 60 µm width and 25 µm depth. Bottom plate thickness was 700 µm

and cover plate thickness was 200 µm. In order to enhance the stability at the capillary-chip couplings two 500 µm glass blocks were bonded at the sides of the capillary inlets (see Figure 1A and 1B). The fused silica capillaries (50 µm ID) were purchased from Polymicro Technologies (Phoenix, AZ), cut to the desired length using a capillary cutter (SHORTIX - Capillary Column Cutter, SGT, The Netherlands and Singapore) and cleaned with isopropanol. GPTMS coating procedure was performed using protocols from literature [30,31]. The glass chip was cleaned in isopropanol upon ultrasonication for 10 min. The coupling was performed by gluing the capillaries to the chip using epoxy glue (Araldite, Huntsman Advanced Materials Ratingen, Germany) as previously reported [32]. All solutions were introduced via port P1 (see Figure 1C). During operation, unused channel ends were blocked with silicone filled CE vials.

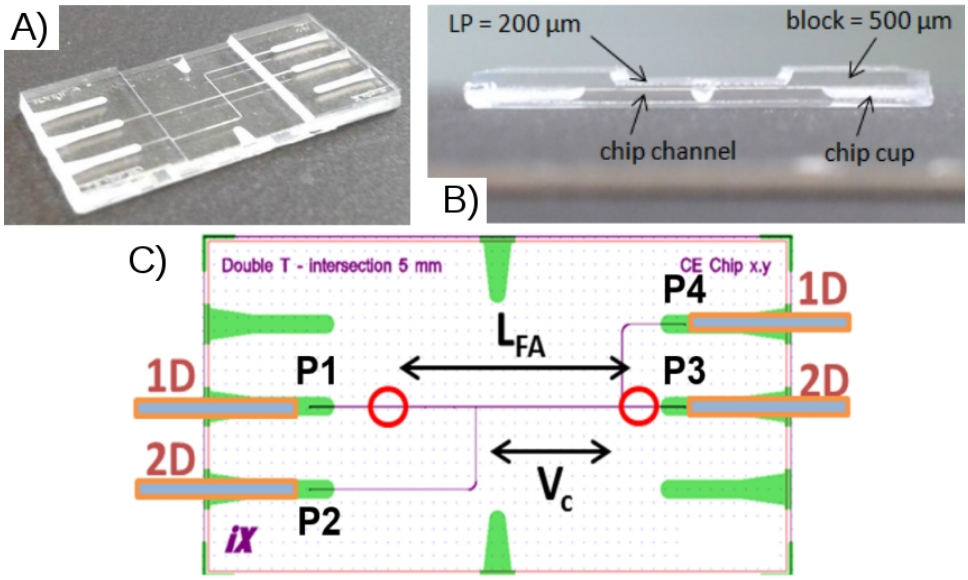

Figure 1: A) general view of a cross layout channel network microfluidic chip. B) Side view of chip interface with channels, and glass blocks for increasing mechanical stability. C): 4-port chip scheme for a double-T layout with 5 mm common intersection segment length (V_c = ~ 7 nl and 5 mm length). L_{FA} = length of the fiber array was 8.75 mm.

Protein labeling

Model proteins were labeled with Chromeo P503 [33-35] from Active Motif (Carlsbad, CA, USA) via mixing 10 µl of protein stock solution (5 mg/ml in water of β-lactoglobulin) with 15 µl of $Na_2B_4O_7$ buffer solution (10 mmol/l, pH 9.2) and 1 µL of P503 labeling solution (2.5 mmol/l in methanol). The labeling reaction took 30 min at room temperature. In order to quench the reaction, 40 µL water was added. Right before the experiment water were added to a final volume of 100 µl [36].

Characterization of the setup

The setup was characterized via a series of flushing experiments using a solution of 2 µg/ml fluorescein isothiocyanate (FITC) in $Na_2B_4O_7$ buffer (10 mmol/l, pH 9.2) and an LED intensity of 98% and an exposure time of 1000 ms (data rate = 1 Hz) for the push broom imager. The FITC solution was flushed from port P1 into the setup and MS detection, if used,

was located at port P3 (Figure 1). The ports P2 and P4 were filled with buffer solution. Between experiments, residual FITC was flushed out with $Na_2B_4O_7$ buffer solution (10 mmol/l, pH 9.2). For the determination of linear range and LOD, FITC solutions with different concentrations (ranging from 0.125 to 50 µg/ml) were flushed through the chip at 100 mbar and detected in the chip interface at an exposure time of 1000 ms (data rate = 1 Hz). The LED intensity was at 98 %. Rinsing with $Na_2B_4O_7$ buffer, pH 9.2 at 2 bar for 600 s was used between measurements.
The time-dependence was tested by pumping two plugs of FITC solution through the interface. For this, the hybrid capillary-microchip setup was first flushed with a buffer of 100 mmol/l formic acid (pH 2.4) for high ionization efficiency in the MS, followed by injecting two plugs of a basic FITC solution (in $Na_2B_4O_7$ buffer, pH 9.2) at a concentration of 0.5 mg/ml (1.28 mmol/l) for 1 s at 1 bar with an intermediate plug of 100 mmol/l formic acid (injected at 1 bar for 12 s). The stack was then flushed through the chip at a pressure of 1 bar from port P1 (with 100 mmol/l formic acid) to the MS detection at port P3 (see Figure 1C). On-chip detection was performed with a detection rate of 1 Hz. MS detection was accomplished with the single quadrupole instrument recording the $[M+H]^+$ ion of FITC at m/z 390.2.

Conditions and parameters for 1D CIEF-LED-IF

The sample was included in a solution containing 2.0 % v/v Pharmalyte 3-10 carrier ampholytes and 0.1 % v/v HEC as a dynamic EOF modifier to minimize EOF velocity [37]. A 1.0 % w/v HEC stock solution was prepared by dissolving 0.4 g HEC in 40 ml doubly-deionized water at 70°C. Anolyte and catholyte were 1 mol/l aqueous acetic acid and 250 mmol/l aqueous triethylamine (TEA) respectively, both containing 0.1 % w/v HEC. The solution with the labeled protein was mixed with the carrier ampholyte stock solution with the final concentration of the model protein of 1 mg/ml. A custom-made multiport HV source (CalvaSens, Aalen, Germany) enabling the independent operation of 12 high voltage channels, 6 positive (from 0 to 15 kV) and 6 negative (from -15 to 0 kV) was used for setting the electric potential regime. Together with a home-made multi-vial unit [29] this enabled the simultaneous and independent control of pressure and high voltage regimes for up to four vials. Pressure application of 1 bar for injection and flushing was achieved via the pneumatic unit of an Agilent 7100 CE system (Agilent Technologies, Waldbronn, Germany) by-passing the pneumatic connection of the inlet port via pneumatic valves Festo MFH-3-M5 (FESTO, Neuss, Germany) controlled manually with an ad-hoc switch module. First, capillaries and chip were rinsed with anolyte (600 s at 1 bar), injection was accomplished for 15 s at 1 bar followed by the injection of a catholyte plug to avoid cathodic drift. The CIEF separations were carried out at -19 kV with detection at the anodic end, applying voltage over capillaries and chip between ports P1 (-10 kV) and P3 (+9 kV) in a double T layout with 5 mm common intersection (see Fig. 1C). The pH gradient was mobilized after 7 min at a pressure of 1 bar keeping the applied voltage. The ports P2 and P4 were hydrodynamically closed and electrically isolated.
LED and FITC fluorescence (c = 2 µg/ml) intensity depended linearly on the LED intensity (set between 20 and 98 % (R^2 = 0.999; 1000 ms). For best LODs, the LED was generally used at maximal intensity of 98 % for all measurements. Likewise, a linear correlation (R^2= of 0.9999) was observed for the dependence on exposure time at FITC concentrations between 0.125-0.1 µg/ml. Saturation of the push broom imager became visible at 70000 counts. Exposure times of 1000 to 2500 ms (data rate = 1.0 to 0.4 Hz) were suitable for on-chip

detection during electrophoretic runs, however, at low analyte concentration, exposure times may be increased up 4500 ms, however with a lower number of data points describing the signal.

Intermediate on-chip LED-IF detection - strategy and realization

Our goal was to precisely monitor the movement of the analyte of interest through the interface to define the ideal time point for voltage-switching for heart-cutting in 2D applications (e.g. CIEF/CE-MS). The ideal way would include imaging of the intersection area, here especially the common intersection for double-T interfaces (of length L_{FA} = 8.75 mm in Figure 1C) with high spatial and temporal resolution. For more complex applications, in addition spectral resolution is of further interest. The following elements of the setup were implemented for on-chip LED-IF detection (a detailed description including schematic drawings can be found in the supplementary material):

i) Excitation of the fluorophore in the common intersection is achieved with LED light collected via a cylindrical lens, which is first parallelized, and then focused onto a small line using a planoconvex lens. The focal area and distances of the lenses were chosen in a way that a channel segment of about 10 mm was covered and the focal point was directly in the middle horizontal plane of the channel. Adjusting the distances between lenses and to the channel, both width and intensity of the illuminated path could be modified. Turning the second lens by 90° enabled spot illumination.

ii) Spatial resolution was achieved on the detection side using a light fiber array imaging the full intersection (length L_{FA}) with 24 optical fibers aligned, ensuring about 10 data points along the channel and an acceptable overlap of light cones. To ensure minimal cross-collection of fluorescence light by two neighboring 100 µm light fibers, several parameters like distance of the light fiber array to the chip surface, the resulting air layer, and the channel-to-surface distance were taken into account. We thus calculated the base width of a light cone from one fiber to the chip channel which is equal to the channel segment covered by detection. The result of this calculation (considering 1500 µm for the air gap due to the extra glass blocks, and 200 µm for the top glass plate) is that the cone has a diameter of 832 µm in the middle plane of the channel. Considering a percentage of 33 % of all fibers being active (24 of 70), this means that between cones an overlap of 457 µm or 50% exists. Considering the case of 17 % of active fibers (12 of 70), the overlap reduces to 82 µm or 10%. No overlap on the detection side was present. As a quantitative information is not required for monitoring the analyte migration in the chip, the overlap is acceptable and assures that no blind parts are present on the chip

The wavelength of the LED was chosen to be universal to excite common low-cost fluorophore labels used for fluorescence detection as for example fluorescein [38] or aminopyrene trisulfonic acid (APTS) [39] and their derivatives, as well as P503 dye especially designed for CIEF [33-36], which was used in this work. These fluorophores have absorption maxima in the range of 440-500 nm. For this reason, a temperature-controlled high power LED with an emission wavelength of 455 nm was chosen as the excitation light source.

The P503 label used in this work is a dye especially designed for labeling proteins in CIEF separation assays with fluorescence detection. Covalently bound to a protein the absorption and emission maxima are at 503 nm and 603 nm respectively. Excitation at 455 nm is at approximately 70 % of the maximum intensity for absorption. The unbound label absorbs only at higher wavelengths and has only very low emission, consequently, no sample cleanup is required after derivatization. A band pass filter was used to reduce the band width of the detection light and a long pass filter to minimize stray light intensity for detection.

Fiber array for collection emission light

In order to develop spatially-resolved on-chip intermediate detection, a hyperspectral push broom imager was used. This detector consists of a spectrograph followed by a CCD camera with a defined active sensor area for the detection in the wavelength range of 380–980 nm. The connection between chip and detector was a linear fiber array, designed jointly with J&M Analytik AG (Essingen) and constructed by art photonics (Berlin, Germany). The fiber array consists of 24 × 80 cm long active UV/VIS light fibers, see Figure 2. For a maximal spatial resolution for the active detection area, light fibers with the technically smallest possible diameter (100 µm, 125 µm including the outer coating) were chosen. Both ends of the fiber array have to assure spatial resolution:

i) at the detector side (LF1, Figure 2): 69 blind and 24 active fibers (93 in total) with a total length of 93 * 125 µm = 11.625 mm were coupled. This allowed keeping spatial resolution but also maximizing the illuminated number of pixels per fiber and thus sensitivity on the active CCD sensor area of the push broom imager (being 11.84 x 8.88 mm (entrance slit width of the push broom imager was 14 mm)). A pixel can be calculated to cover 5.5 µm of the sensor area, one light fiber illuminates 23 pixels.
ii) at the chip side (LF2, Figure 2): The channel segment of about 9 mm was imaged using the 24 active fibers separated by 46 blind fibers defining the spatial distance between them resulting in a total width of 70 * 125 µm = 8.750 mm. Using all active fibers 10 data points with an overlap of about 457 µm or 5 data points using only every second active fiber with an overlap of only 82 µm were obtained.
Using this combination, the spectral information collected by each single light fiber of the linear fiber array is projected onto the CCD chip without overlap, giving rise to a spatially-resolved image of a channel segment of 9 mm length. For the particular layout shown here, 5 mm of such length cover the common intersection and the additional 1-3 mm allow additional monitoring, especially before the analyte migrates into the intersection. It is important to note that the order of the active fibers was preserved from chip to detector side. Due to the coupling into the push broom imager one of the outer light guides is not perfectly included into the active CCD array of the push broom imager and therefore only 23 light guides are actually usable.

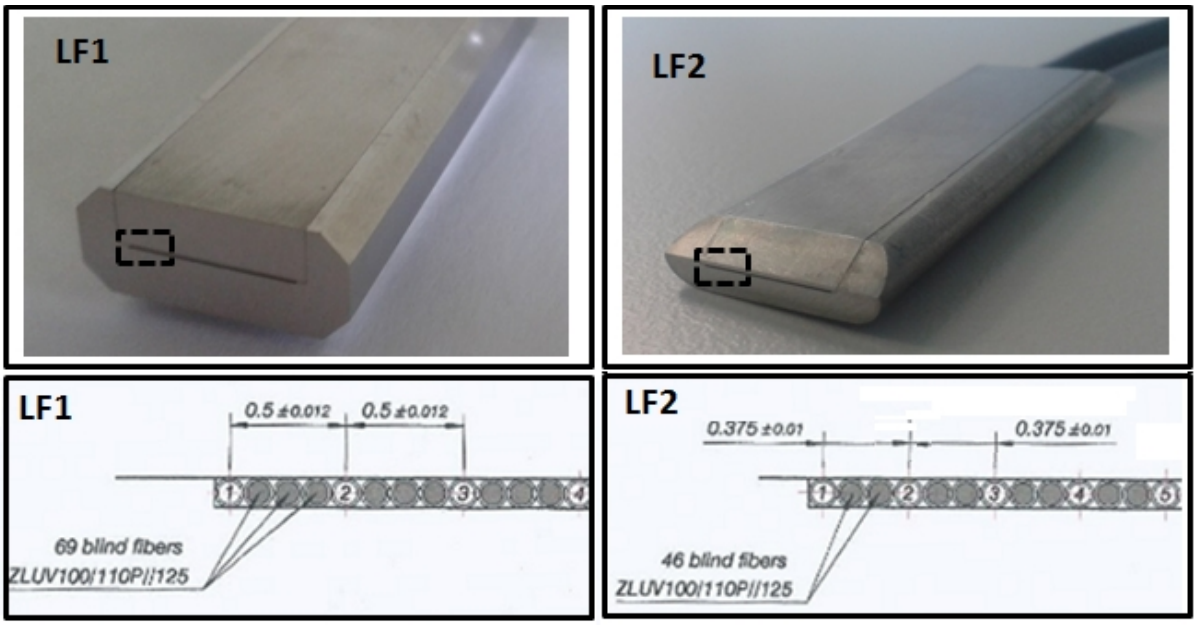

Figure 2: Illustrations of the push broom side (LF1) as well as on-chip detection side (LF2) of the constructed fiber array. Bottom drawings are modified CAD files from art photonics GmbH (Berlin, Germany).

Hyperspectral imaging - Push broom imager as detector

Hyperspectral imaging was initially developed for remote sensing of the earth's surface [40]. Currently, due to its great potential, it has been implemented in a plethora of scientific fields like agriculture, pharmaceutical and material science as well as food quality and safety applications [41]. Using the push broom imager in spatial scanning mode it can record a time dependent full spectrum (e.g. 380 nm – 980 nm) over a defined array length and therefore it generates a 4D signal: intensity, space, wavelength and time resolved. The detection setup used in this work as well as the software used to record and display data were developed in cooperation with J&M Analytik AG (Essingen, Germany). Further information on specifications and custom-made control software are given in the supplementary material. The exposure time was adapted between 500 to 5000 ms to adjust the SNR. With the temporal peak widths of 6 to 15 s for CE and 20 to 40 s in CIEF, the exposure time was lowered to 0.2 Hz to adequately describe the electrophoretic signals.
Figure 3A demonstrated the spatial and wavelength resolution of the detection system using a hyperspectral plot with intensities of the excitation light (455 nm LED) and FITC solution (2 µg/mL) fluorescence (520 nm) flushed through the channels. All 23 active light guides can be evaluated. The optical spectrum and intensity distribution for all fibers are given in Figure 3B and C (see red cursor lines for Fiber #10, and for 450 nm, in Figure 3A). Also, time-dependent imaging is possible for all or selected light fibers. The custom-made software allows simultaneous spectral and spatial monitoring over time.

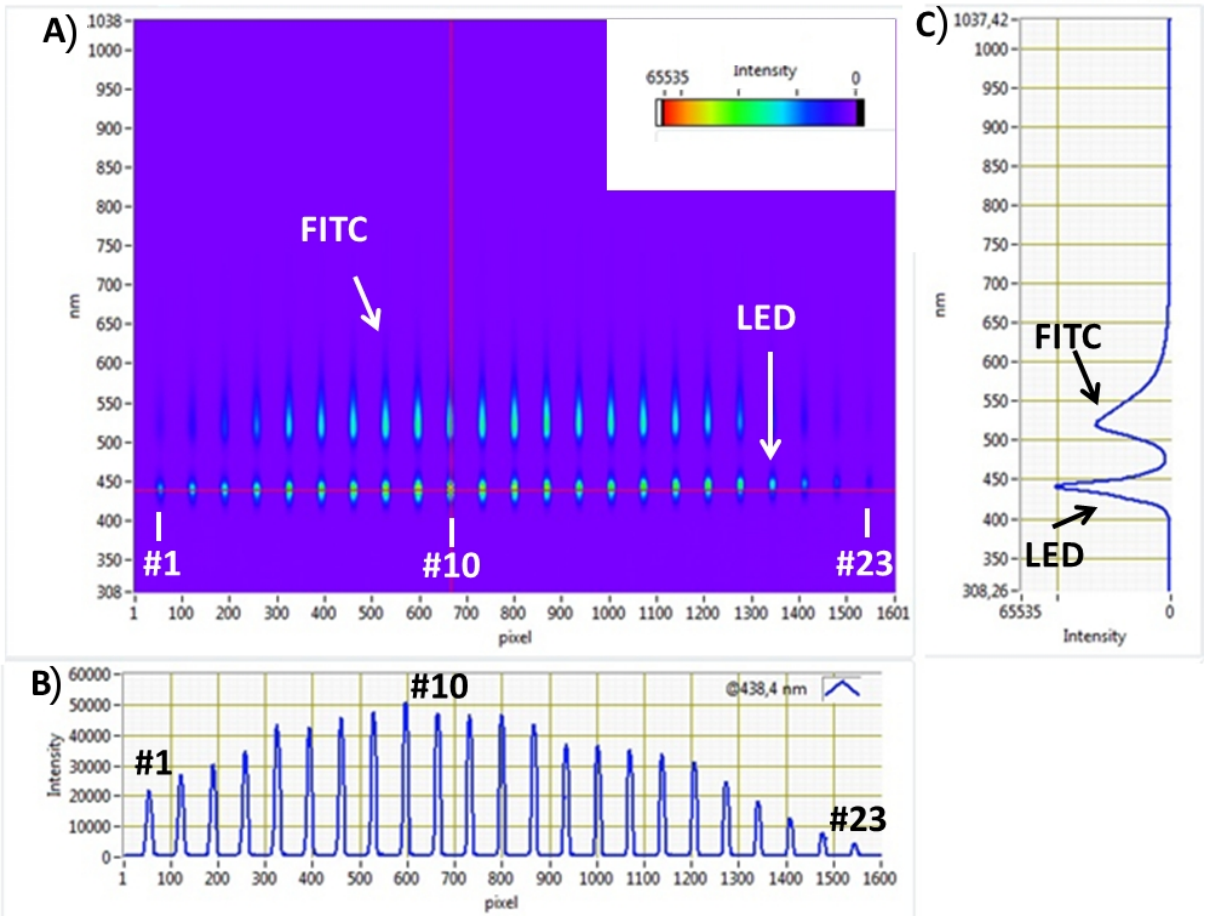

Figure 3: Monitoring option of the push broom imager: ***A)*** *three dimensional hyperspectral plot for the 23 active light guides,* ***B)*** *spatially-resolved fluorescence signal for a chosen wavelength with respect to exposed pixels of the CCD camera of the push broom imager and* ***C)*** *the spectral plot for the wavelength range of 308 to 1037 nm for the chosen position (vertical red cursor line). Concentration of the FITC solution was 2.0 µg/ml.*

Characterization of the fluorescence detection setup

Quality and performance of light fiber array

The homogeneity of excitation and detection of fluorescence light was determined using thin layer chromatography (TLC) plates homogeneously immersed in FITC solution, which were placed under the detection setup instead of a microfluidic chip. The resulting intensity distribution for all light guides in the excited range of about 6 mm width shows the high quality of the proposed setup, clearly sufficient for accurately monitoring the migration of analytes inside the microchannel. At high exposure time, very good SNR were obtained. Line vs. point detection is possible by adjusting the appearance of the excitation line just by turning the optical shell by 90° (see Figure 4) to reach an illuminated spot of only 1.8 x 8 mm². The

appearance of the illuminated area can further be varied changing the optical path length between the cylindrical lens and the chip. A larger distance leads to a larger area being illuminated but also to a lower intensity.

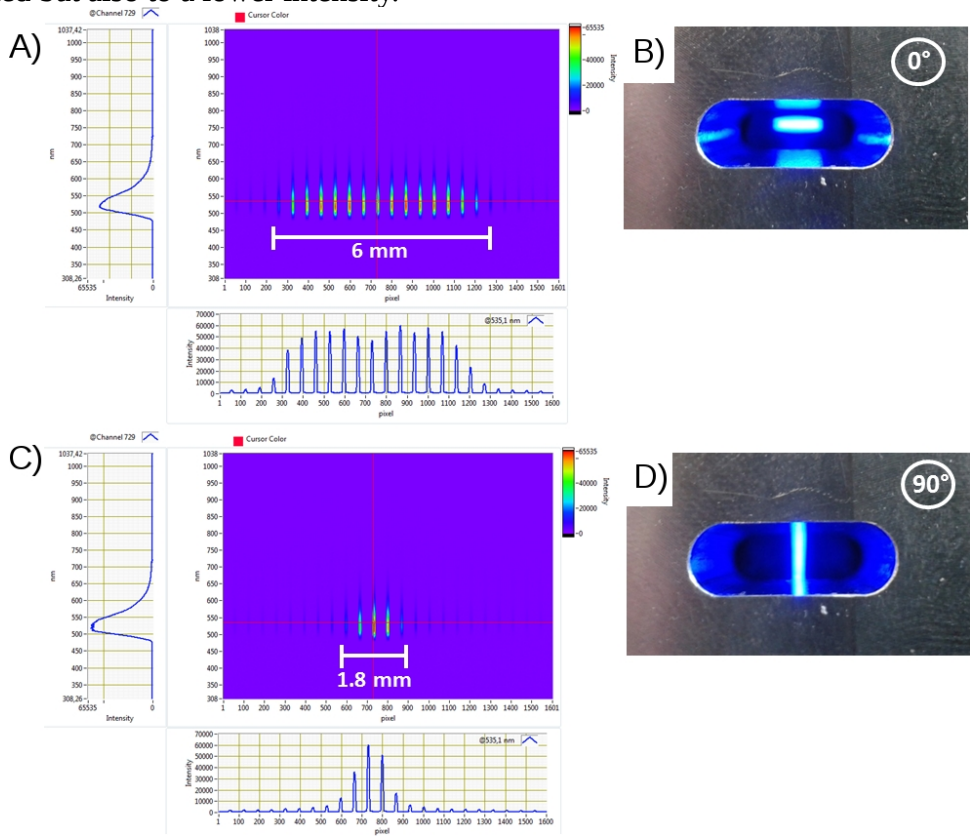

Figure 4: A) Hyperspectral plot for the linear (0° angle) excitation arrangement. B) Appearance of the excitation light beam in the focal point of the optical geometry. C) Hyperspectral plot for the linear (90° angle) excitation arrangement. D) Appearance of the excitation light beam in the focal point of the optical geometry. Experiments were done for a TLC plate immersed in an FITC solution.

For linear range and LOD determination flushing experiments were conducted in triplicate. RSD valued were below 1%. The calibration curve was linear for FITC solution of 0.125 to 25 µg/ml (R^2 = 0.999). At higher concentration asymptotic behavior was observed, most likely due to fluorescence saturation and quenching effects [42].

At a concentration of 0.125 µg/ml (0.32 µmol/l) of FITC, an SNR of 4 was observed. The detection volume inside the channel is only 1.2 nl for each light fiber and thus an equivalent absolute LOD of only 0.04 fmol was reached for a single fiber. It is worth to mention, that this LOD reached with the presented setup is comparable to those reported in the literature, in the order of some attomoles [12,43,44]. Nevertheless, is even more important to point out, that those works employed laser technology for the excitation, instead of LED as it is tha case of the presented setup. Clearly, with a more portable and affordable system, the reached similar LOD, positions this setup as advantageous for intensive use in the laboratory. Another extra advantage, is the possibility of the wavelength resolution that is only possible with LED source.

Chip positioning and alignment procedure for in channel measurements

No difference in light intensity was observed whether detection was accomplished at the top side of the chip (Mode A) or from the bottom with the etched curved channel side (Mode B) facing the excitation light path. Most likely this is due to the equal overall distance between channel and fiber array [12,22] of 1700 µm, differing only in the ratio of glass vs. air (see supplementary material). Due to this, a single optical fiber is able to monitor a channel segment of 832 (Mode A) and 851 µm (Mode B), respectively.
In order to assure an optimal positioning of the microfluidic channel in the light path of the fiber array after the assembly of the setup, additional effects on the fluorescence intensity of specific light fibers can be used. These effects consist of increased intensities due to channel cross sections and reflection at the edges of the additional glass blocks used for stabilizing the capillary chip cups. For the alignment procedure, the channel was flushed with fluorophore. Figure 5 shows the intensity distribution over all light fibers for both Modes A and B, changing the relative position of the chip (right R and left L) and thus the segment being monitored. As can be deduced from Figure 2, the channel cross section evokes an intensity increase for both detection Modes A and B as well as for right or left positioning. This is well corroborated by the photographs of the visual light beam line with the cross section marked by the white star. In addition, in Figure 2C and D the reflection from the bonded glass blocks was observed at light guides #6 and #7 or #18 and #19 (counting from left), respectively.

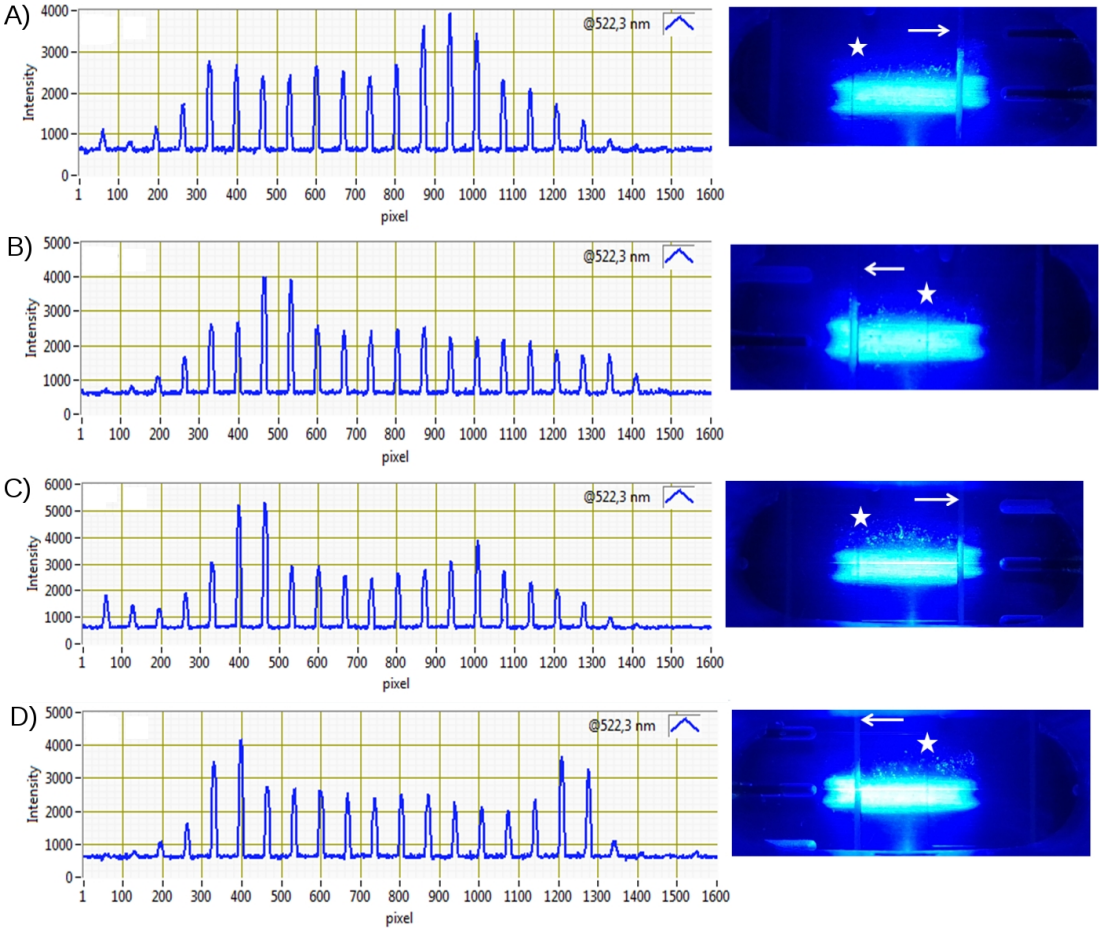

Figure 5: Recorded detector signals for each light guide of the fiber array as well as photographs of the light beam line of the excitation light for detection Mode A (A and B) and Mode B (C and D). The chip was moved to the left (Figure 5A and C) and right (Figure 5B and D) relative to the surface edge of the additionally bonded 500 µm glass block. The white star indicates the position of the chip

channel intersection (here, for a cross layout) and the white arrow indicates the position of the surface edge of the additionally bonded 500 µm glass block.

Due to the increased information regarding the chip position, detection Mode B was chosen for all further experiments. The clear alignment allows to choose monitoring parts of the migration path preferably prior or after the intersection. The current setup would thus allow simultaneous fluorescence monitoring through the bottom plate and conductivity detection through the thin cover plate using contactless conductivity detection [28,29].

On-chip monitoring of CIEF-focused P503 labeled protein

Finally, in order to test the on-chip LED-IF detection system for monitoring electrophoretic separations, a classical CIEF assay was performed in the first separation dimension using the 2D setup with pressure mobilization after the focusing step to flush the analyte (P503-labeled ß-lactoglobulin) through the LED-IF detection system. After 7 min of focusing, the ampholyte stack was mobilized using 100 mbar pressure applied to port P1 of the setup and the optical on-chip detection was started. The labeled protein was detected in the chip interface after 7 min with a peak width of 40 s (see Figure 6). The slight tailing of the peak is due to the relatively high concentration of the protein of 2 mg/ml chosen here to fully demonstrate the monitoring capabilities and describe the movement of the analyte band inside the chip interface. Figure 6A and B show the hyperspectral plot and the fluorescence spectrum for LED stray light and the protein (for light fibers #2 to #8) at t = 7 min. Figure 6C shows the electropherogram for the protein over selected light guides. Clearly, the movement through the chip with a very precise information of the analyte position can be followed taking into account the light intensity for different light fibers and thus at different position in the channel. Figure 6 thus impressively demonstrates the temporal, spatial and wavelength resolution possibilities of the presented LED-IF setup.

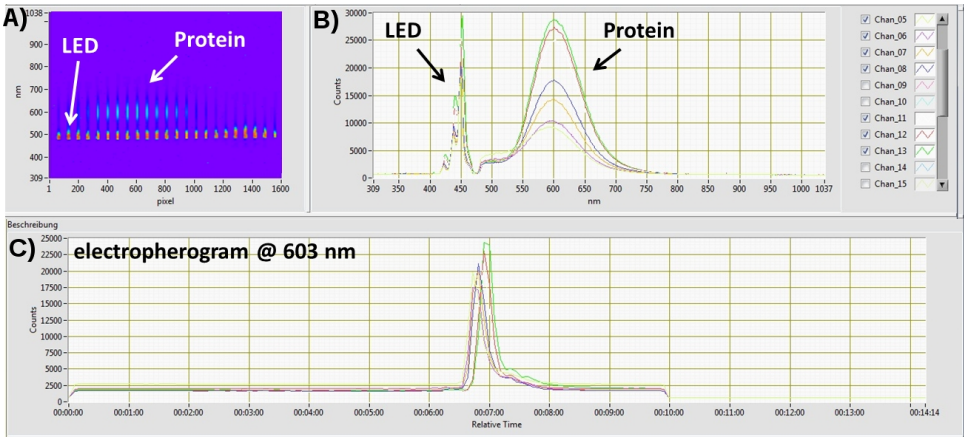

Figure 6: On-chip LED-IF detection of P503 labeled ß-lactoglobulin by CIEF with pressure mobilization. All three diagrams of the hyperspectral software of the push broom imager are shown. ***A****) the hyperspectral plot for t = 7 min,* ***B)*** *the spectral plot in detail and* ***C)*** *the time dependent signal recording (here at 603 nm) of the fluorescence signal for each active light guide of the fiber array. Light guide intensities plotted in* ***A)*** *and* ***B)*** *for fibers 2-8.*

These resolution changes can also be followed using the hyperspectral image at different time points (420, 428, 436 and 444 s) of the separation when the protein enters the chip interface as shown in Figure 7. The peak width and changes in the peak shape can nicely be monitored via

the hyperspectral plot. A spatial peak width of 3.5 mm with the signal spreading over about half of the channel image can be determined. Clearly, the setup is suitable for intermediate (or final) detection of CIEF focused labeled protein and can be used to monitor on-chip analyte band transfer from the first to the second separation dimension and determine the optimal time point for voltage switching in 2D applications.

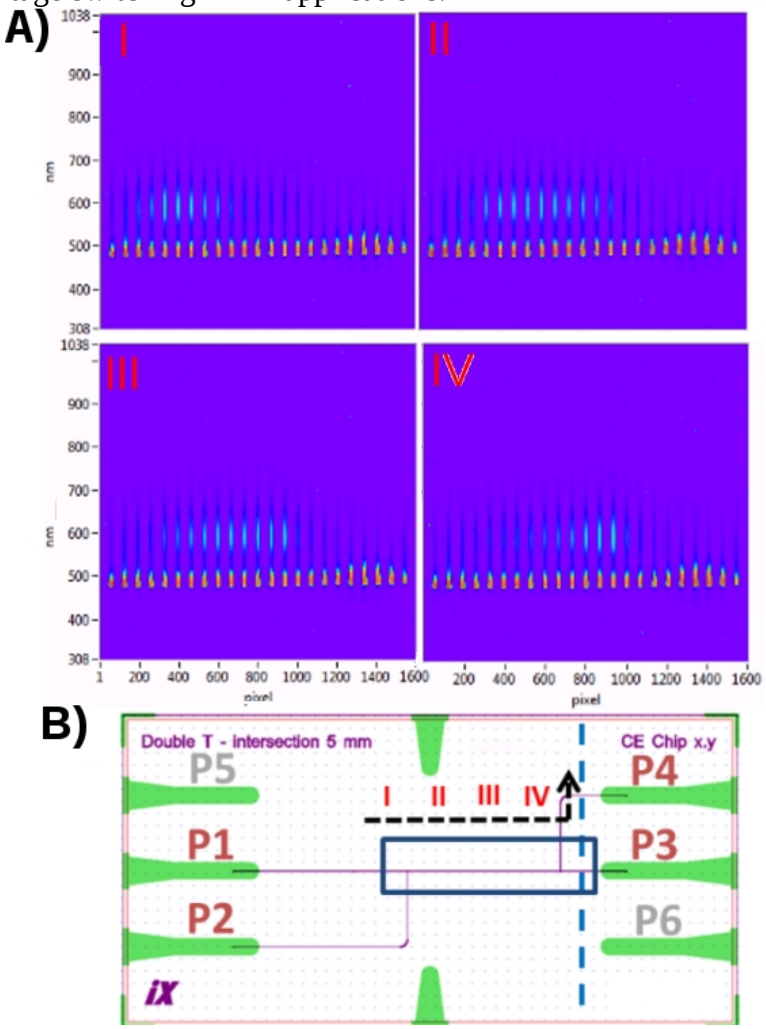

*Figure 7: **A)** Time-dependent recording via hyperspectral imaging plots shown for time points 420 (I), 428 (II), 436 (III) and 444 s (IV) of the protein moving through the chip interface after CIEF focusing by applying 100 mbar from ports P1 to P4. The ports P2 and P4 were hydrodynamically closed using silicone-filled vials. **B)** Relation of time points to the position of the protein in the chip. The blue square shows the imaged part of the interface via the LED-IF detection setup. The dashed black line gives the flow direction of the protein sample band through the interface. The slight increase for the excitation light at ca. 500 nm for light fibers situated at the end of the migration path is due to reflection phenomena at the surface edge of the additionally bond 500 µm glass block.*

Conclusion

A spatially-resolved intermediate on-chip LED-IF detection system was successfully implemented for a hybrid microfluidic capillary-chip glass interface. The setup includes a high power 455 nm LED prototype as excitation light source and a linear light fiber array

consisting of 23 active 100 µm light fibers for spatially-resolved fluorescence detection in combination with a push broom imager for hyperspectral imaging. The optical parts were arranged in a bevel angle setup with the excitation light focused at an angle of 45° and fluorescence detection perpendicular to the chip surface. Absolute detection limits of 0.04 fmol were obtained considering the very small detection volumes. The modular setup proved to be very flexible: i) it is applicable both for in-channel detection as well as for solid samples (contaminated TLC plates); ii) the appearance of the excitation light beam can be varied changing the optical path length and switching from line to spot detection; iii) different excitation sources can be implemented due to the use of fiber optics; iv) the chip position can be varied according to the needs of the separation with a well-controlled alignment.

The optical on-chip detection therefore allows a precise control of analyte migration and thus a precise sample transfer between different separation dimensions. Simultaneous temporal, spatial and wavelength recording is possible with the developed custom-made software.

Conflict of interest

The authors declare no conflict of interest.

Acknowledgement

This work was funded by the Excellence Initiative, a jointly funded program of the German federal and state governments, organized by the German Research Foundation (DFG).

References

[1] Kler PA, Sydes D, Huhn C. Column–coupling strategies for multidimensional electrophoretic separation techniques. Anal Bioanal Chem. 2015; 407 (1): 119-138.
[2] Lamari, FN, Kuhn, R, Karamanos, NK. Derivatization of carbohydrates for chromatographic, electrophoretic and mass spectrometric structure analysis. J. Chromatogr. B. 2003; 793 (1), 15-36.
[3] Wu J, Pawliszyn J. Capillary isoelectric focusing with a universal concentration gradient imaging system using a charge-coupled photodiode array .Anal. Chem. 1992; 64: 2934-2941.
[4] Chiang MT, Chang SY, Whang CW. Analysis of baclofen by capillary electrophoresis with laser-induced fluorescence detection. J. Chromatogr. A. 2000; 877: 233-237.
[5] Horká M, Willimann T, Blum M, Nording P, Friedl Z, Šlais K. Capillary isoelectric focusing with UV-induced fluorescence detection .J. Chromatogr. A. 2001; 916: 65-71.
[6] Schwarz MA, Hauser PC. Recent developments in detection methods for microfabricated analytical devices. Lab Chip 2001;1: 1–6.
[7] Lin YW, Chiu TC, Chang HT. Laser-induced fluorescence technique for DNA and proteins separated by capillary electrophoresis. J. Chromatogr. B. 2003;793: 37–48.

[8] Liu Z, Pawliszyn J. Capillary isoelectric focusing of proteins with liquid core waveguide laser-induced fluorescence whole column imaging detection. Anal. Chem. 2003;75: 4887-4894.
[9] Götz S, Karst U. Recent developments in optical detection methods for microchip separations. Anal. Bioanal. Chem. 2007;387: 183-192.
[10] Jung B, Zhu Y, Santiago JG. Detection of 100 aM fluorophores using a high-sensitivity on-chip CE system and transient isotachophoresis. Anal. Chem. 2007;79: 345-349.
[11] Liu Z, Lemma T, Pawliszyn J. Capillary isoelectric focusing coupled with dynamic imaging detection: A one-dimensional separation for two-dimensional protein characterization. J. Proteome Res. 2006; 5: 1246-1251.
[12] Fu JL, Fang Q, Zhang T, Jin XH, Fang ZL. Laser-induced fluorescence detection system for microfluidic chips based on an orthogonal optical arrangement. Anal. Chem. 2006; 78: 3827-3834.
[14] Dada OO, Ramsay LM, Dickerson JA, Cermak N, Jiang R, Zhu C, Dovichi NJ. Capillary array isoelectric focusing with laser-induced fluorescence detection: milli-pH unit resolution and yoctomole mass detection limits in a 32-channel system. Anal. Bioanal. Chem. 2010; 397: 3305–3310.
[15] Ramsay LM, Dickerson JA, Dada O, Dovichi NJ. Femtomolar concentration detection limit and zeptomole mass detection limit for protein separation by capillary isoelectric focusing and laser-induced fluorescence. Anal. Chem. 2009; 81: 1741–1746.
[16] Huhn C, Pütz M, Pyell U. Separation of very hydrophobic analytes by micellar electrokinetic chromatography. III. Characterization and optimization of the composition of the separation electrolyte using carbon number equivalents. Electrophoresis. 2008; 29: 783–795.
[17] Ryvolova M, Macka M, Preisler J. Portable capillary-based (non-chip) capillary electrophoresis. Trac-Trend Anal. Chem. 2010; 29: 339-353.
[18] Tong W, Yeung ES. Simple double-beam absorption detection systems for capillary electrophoresis based on diode lasers and light-emitting diodes. J Chromatogr. A. 1995; 718: 177-185.
[19] Xiao D, Zhao S, Yuan H, Yang X. CE detector based on light-emitting diodes. Electrophoresis. 2007; 28: 233–242.
[20] Xiao D, Yan L, Yuan H, Zhao S, Yang X, Choi MMF. CE with LED-based detection: An update. Electrophoresis. 2009; 30: 189–202.
[21] Chabinyc ML, Chiu DT, McDonald JC, Stroock AD, Christian JF, Karger AM, Whitesides GM. An integrated fluorescence detection system in poly (dimethylsiloxane) for microfluidic applications. Anal. Chem. 2001; 73: 4491-4498.
[22] Sluszny C, He Y, Yeung ES. Light-emitting diode-induced fluorescence detection of native proteins in capillary electrophoresis. Electrophoresis. 2005; 26: 4197–4203.
[22] Liu C, Mo YY, Chen ZG, Li X, Li OL, Zhou X. Dual fluorescence/contactless conductivity detection for microfluidic chip. Anal. Chim. Acta. 2008; 621: 171–177.
[23] Novak L, Neuzil P, Pipper J, Zhang Y, Lee S. An integrated fluorescence detection system for lab-on-a-chip applications. Lab Chip. 2007; 7: 27–29.
[24] Wu J, Pawliszyn J. Absorption spectra and multicapillary imaging detection for capillary isoelectric focusing using a charge coupled device camera. Analyst. 1995; 120: 1567-1571.
[25] Beck W, van Hoek R, Engelhardt H. Application of a diode-array detector in capillary electrophoresis. Electrophoresis. 1993: 14: 540-546.
[26] Schäferling M. The art of fluorescence imaging with chemical sensors. Angew. Chem. Int. Ed. 2012; 51: 3532–3554.

[27]Liu Z, Pawliszyn J. Applications of capillary isoelectric focusing with liquid-core waveguide laser-induced fluorescence whole-column imaging detection. Anal. Biochem. 2005; 336, 94-101.
[28] Kler PA, Posch TN, Pattky M, Tiggelaar RM, Huhn C. Column coupling isotachophoresis–capillary electrophoresis with mass spectrometric detection: Characterization and optimization of microfluidic interfaces. J. Chromatogr. A. 2013; 1297: 204–212.
[29] Kler PA, Huhn C. Non-aqueous electrolytes for isotachophoresis of weak bases and its application to the comprehensive preconcentration of the 20 proteinogenic amino acids in column-coupling ITP/CE–MS. Anal. Bioanal. Chem. 2014; 406: 7163–7174.
[30] Shao X, Shen Y, O´Neill K, Lee ML. Capillary electrophoresis using diol-bonded fused-silica capillaries. J. Chromatogr. A 1999; 830: 415-422.
[31] Horká M, Willimann T, Blum M, Nording P, Friedl Z, Šlais K. Capillary isoelectric focusing with UV-induced fluorescence detection. J. Chromatogr. A. 2001; 916: 65-71.
[32] Tiggelaar R, Benito-Lopez F, Hermes D, Rathgen H, Egberink R, Mugele F, Reinhoudt D, van den Berg A, Verboom W, Gardeniers H. Fabrication, mechanical testing and application of high-pressure glass microreactor chips. Chem. Eng. J. 2007;131: 163–170.
[33] Craig DB, Wetzl BK, Duerkop A, Wolfbeis OS. Determination of picomolar concentrations of proteins using novel amino reactive chameleon labels and capillary electrophoresis laser-induced fluorescence detection. Electrophoresis 2005; 26: 2208–2213.
[34] Wetzl BK, Yarmoluk SM, Craig DB, Wolfbeis OS. Chameleon labels for staining and quantifying proteins. Angew. Chem. Int. Ed. 2004; 40: 5400–5402.
[35] Wojcik R, Swearingen KE, Dickerson JA, Turner EH, Ramsay LM, Dovichi NJ. Reaction of fluorogenic reagents with proteins: I. Mass spectrometric characterization of the reaction with 3-(2-furoyl)quinoline-2-carboxaldehyde, Chromeo P465, and Chromeo P503. J. Chromatogr. A, 2008; 1194: 243–248.
[36] Dickerson JA, Ramsay LM, Dada OO, Cermak N, Dovichi NJ. Two-dimensional capillary electrophoresis: Capillary isoelectric focusing and capillary zone electrophoresis with laser-induced fluorescence detection. Electrophoresis.2010; 31: 2650–2654.
[37] Verzola B, Gelfi C, Righetti PG. Quantitative studies on the adsorption of proteins to the bare silica wall in capillary electrophoresis: II. Effects of adsorbed, neutral polymers on quenching the interaction. J. Chromatogr. A. 2000; 874: 293-303.
[38] Sjöback R, Hygren J, Kubista M. Quantitative spectral analysis of multicomponent equilibria. Anal. Chim. Acta. 1995; 302: 121-125.
[39] Evangelista RA, Liu MS, Chen FTA. Characterization of 9-aminopyrene-1, 4, 6-trisulfonate derivatized sugars by capillary electrophoresis with laser-induced fluorescence detection. Anal. Chem. 1995; 67: 2239-2245.
[40] Goetz AFH, Vane G, Solomon JE, Rock BN. Imaging spectrometry for earth remote sensing. Science 1985; 228: 1147-1153.
[41] Dale LM, Thewis A, Boudry C, Rotar I, Dardenne P, Baeten V, Fernández Pierna JA Hyperspectral imaging applications in agriculture and agro-food product quality and safety control: a review. Appl. Spectrosc. Rev. 2013; 48: 142-159.
[42] Woltmann E, Meyer H, Weigel D, Pritzke H, Posch TN, Kler PA, Schürmann K, Roscher J, Huhn C. Applicability of UV laser-induced solid-state fluorescence spectroscopy for characterization of solid dosage forms. Anal. Bioanal. Chem. 2014; 406: 6347-6362.
[43]Nickerson B, Jorgenson JW. High speed capillary zone electrophoresis with laser induced fluorescence detection. J High Res Chromatogr. 1988; 11(7): 533-534.

[44] Wu X, Wu J, Pawliszyn, J. Fluorescence imaging detection for capillary isoelectric focusing. Electrophoresis. 1995; 16(1): 1474-1478.